

# What Are the Radical Intermediates in Oxidative N-Heterocyclic Carbene Organocatalysis?

Vianney Regnier,<sup>†</sup> Erik A. Romero,<sup>‡</sup> Florian Molton,<sup>†</sup> Rodolphe Jazzar,<sup>‡</sup><sup>ID</sup> Guy Bertrand,<sup>\*,‡</sup><sup>ID</sup> and David Martin<sup>\*,†</sup><sup>ID</sup>

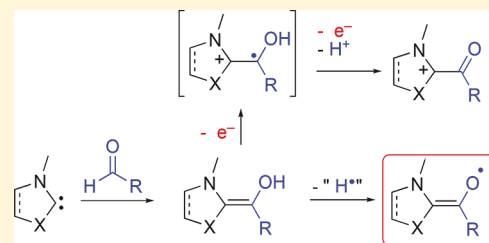
<sup>†</sup>Univ. Grenoble Alpes, CNRS, DCM, 38000 Grenoble, France

<sup>‡</sup>UMI CNRS 3555, Department of Chemistry and Biochemistry, University of California, San Diego, La Jolla, California 92093-0343, United States

## Supporting Information

**ABSTRACT:** The oxidation of the Breslow intermediate resulting from the addition of an *N*-heterocyclic carbene (NHC) to benzaldehyde triggers a fast deprotonation, followed by a second electron transfer, directly affording the corresponding acylium at  $E > -0.8$  V (versus  $\text{Fc}/\text{Fc}^+$ ). Similarly, the oxidation of the cinnamaldehyde analogue occurs at an even higher potential and is not a reversible electrochemical process. As a whole, and contrary to previous beliefs, it is demonstrated that Breslow intermediates, which are the key intermediates in NHC-catalyzed transformations of aldehydes, cannot undergo a single electron transfer (SET) with mild oxidants ( $E < -1.0$  V).

Moreover, the corresponding enol radical cations are ruled out as relevant intermediates. It is proposed that oxidative NHC-catalyzed radical transformations of enals proceed either through SET from the corresponding electron-rich enolate or through coupled electron–proton transfer from the enol, in any case generating neutral captodative radicals. Relevant electrochemical surrogates of these paramagnetic species have been isolated.



## INTRODUCTION

The role of thiazolin-2-ylidene **A** in the active site of thiamine-dependent decarboxylase enzymes,<sup>1</sup> as well as their ability to catalyze benzoin condensation and Stetter-type reactions, have been recognized since the mid-20th century.<sup>2</sup> In 1958, the formation of the so-called Breslow intermediates **IH** was proposed to account for the umpolung transformation of aldehydes into nucleophilic species (Scheme 1).<sup>1,3</sup> Since these pioneering works, the use of stable *N*-heterocyclic carbenes (NHCs)<sup>4–6</sup> as organocatalysts, especially 1,2,4-triazol-3-ylidene **B**, has grown exponentially.<sup>6</sup>

The scope of this rich chemistry has been even further broadened through the use of oxidative conditions. An alternative biomimetic approach was inspired by thiamine-based oxidoreductases, in which the Breslow intermediate can undergo a two-electron oxidation and proton transfer to afford acyliums **I**<sup>+</sup>. Because the latter are activated electrophiles, the overall process allows for a variety of oxidative substitutions of aldehydes and related substrates.<sup>6,7</sup> Concomitantly, one-electron oxidations have also been proposed. For instance, NHC-catalyzed reductive coupling reactions,<sup>8,9</sup> in which aldehydes are used as stoichiometric reductants, as well as enantioselective oxidative NHC-catalyzed transformations of enals into  $\beta$ -hydroxyesters,<sup>10</sup> cyclopentanones,<sup>11</sup> and spirocyclic- $\gamma$ -lactones,<sup>12</sup> are believed to proceed through radical pathways. In all cases, the proposed catalytic cycles proceed through a single electron transfer (SET) from the Breslow intermediates **IH** (or **I**<sup>+</sup> in the case of enals) to a mild one-electron oxidant; the resulting radical cations **IH**<sup>•+</sup> (or **I**<sup>•+</sup>)

are regarded as key intermediates, although they have never been spectroscopically observed (Scheme 2).

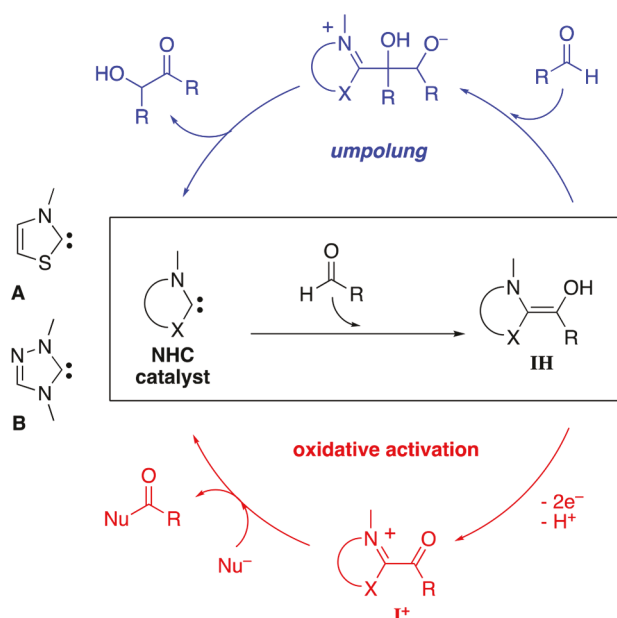
The hypothesized persistency of radical cations **IH**<sup>•+</sup> and **I**<sup>•+</sup> conflicts with mechanistic and electrochemical investigations of standard enols<sup>13</sup> and phenols.<sup>14</sup> Indeed, upon one-electron oxidation, these substrates usually give rise to highly acidic radical cations, which are elusive intermediates and undergo fast deprotonation prior to any further transformation.<sup>13d</sup> Thus, although EPR experiments provided evidence for the formation of radicals during NHC-promoted benzoin condensations, only neutral (amino)(carboxy) C-centered radicals related to **I**<sup>•</sup> (Scheme 3) could be unambiguously identified.<sup>15,20</sup> Note that even the well-accepted Breslow intermediates had eluded observation<sup>16,17</sup> until 2012, when Berkessel et al. finally reported the isolation and X-ray structure of the less reactive (amino)enols **1aH** and **2aH**.<sup>18</sup>

Herein, capitalizing on our previous works on NHC-based captodative radicals,<sup>19</sup> we attempt to assess the structure of key radical intermediates in the oxidative NHC-catalyzed reactions. We rule out the possibility of direct SET from **IH** and **I**<sup>+</sup> to mild oxidants and show that the formation of a significant amount of **IH**<sup>•+</sup> and **I**<sup>•+</sup> is unlikely. We also propose isolable models as redox surrogates for the more relevant neutral radicals **I**<sup>•</sup>.

Received: November 7, 2018

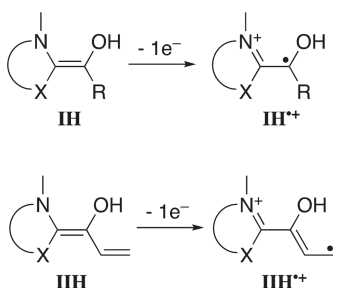
Published: December 18, 2018

**Scheme 1.** Breslow Intermediates IH Are Formed by Reacting an NHC with an Aldehyde<sup>a</sup>



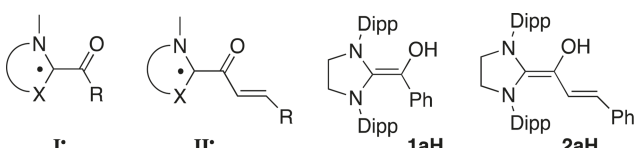
<sup>a</sup>They are involved in the benzoin condensation (in blue) and oxidative nucleophilic substitution of aldehydes (in red).

**Scheme 2.** Postulated Single Electron Transfer (SET) from Breslow Intermediates of Types IH and IIH<sup>a</sup>



<sup>a</sup>The corresponding radical intermediates IH•+ and IIH•+ have been regarded as key intermediates in NHC-catalyzed radical reactions.

**Scheme 3.** Neutral (Amino)(carboxy) C-Centered Radical I•, and Enols 1aH and 2aH That Are Isolable Surrogates for IH and IIH, Respectively<sup>a</sup>



<sup>a</sup>Dipp = 2,6-*i*Pr<sub>2</sub>[C<sub>6</sub>H<sub>3</sub>].

## RESULTS AND DISCUSSION

Our study was prompted by a report from the Rehbein group stating that 1aH coexists with a paramagnetic compound,<sup>20</sup> which they hypothesized to be 1aH•+, based solely on the EPR signal. We prepared the same (amino)enol 1aH and observed the same EPR signal; however, we quickly recognized the hyperfine signature of radical 1a•, a compound that we had previously synthesized by reduction of the corresponding acylium 1a<sup>+</sup> (Scheme 4, Figure 1).<sup>19d</sup>

**Scheme 4.** Synthesis of 1aH from NHC 3 with 1a• as the Paramagnetic Impurity, the Latter Being Quantitatively Prepared by Reduction of 1a<sup>+</sup>

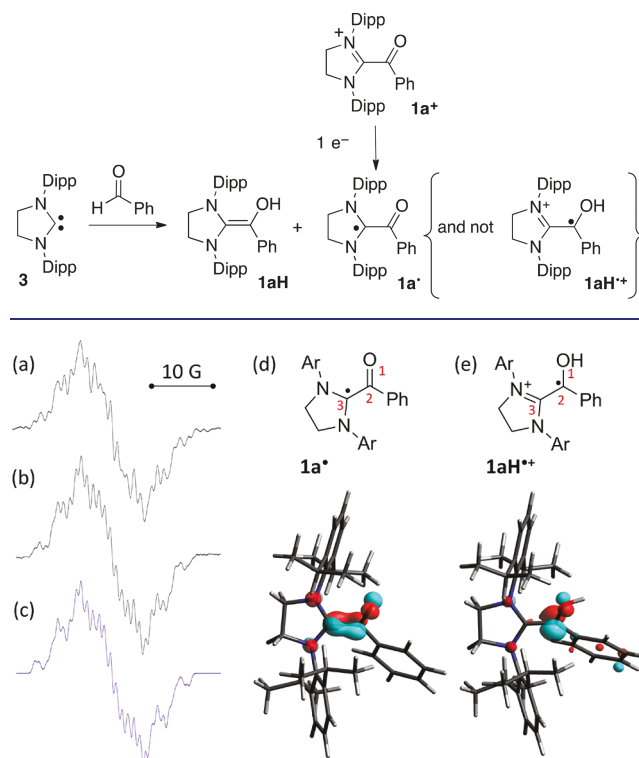


**Figure 1.** (a) Experimental X-band EPR spectra of a freshly prepared solution of 1aH in tetrahydrofuran at room temperature; (b) experimental X-band EPR spectra of a solution of 1a• in dichloromethane at room temperature (prepared by reduction of 1a<sup>+</sup>); (c) simulated band shapes with the following hyperfine coupling constants:  $a(^{15}N) = 6.6$  and 5.4 MHz,  $a(^1H) = 10.66$  (2 nuclei), 8.30 (2 nuclei), 1.49, 2.08, and 3.21 MHz; (d) representation of the singly occupied molecular orbital (SOMO) of 1a•; and (e) representation of the SOMO of 1aH•+.

We performed DFT calculations at the uB3LYP/TZVP level of theory,<sup>21–23</sup> which showed that 1a• and 1aH•+ should have very different EPR signals (Figure 1). Radical 1a• is a typical (amino)(carboxy)radical with 40% Mulliken spin density on the C3 carbon atom with the remaining density spread over the p-system (O1, 30%; C2, 10%; C3, 40%; N atoms, 15%). The predicted isotropic EPR hyperfine coupling constants for 1a• fit well with the experimental values.<sup>19d,24</sup> In marked contrast, for 1aH•+, significant spin density is located on the carbon C2 linked to the hydroxyl group (O1, 10%; C2, 51%, C3, 7%, N atoms, 16%).

The identity of the paramagnetic impurity was further confirmed by detection of the characteristic absorption for 1a• at 540 nm by UV-vis spectroscopy. Freshly prepared solutions of 1aH are light yellow, indicating the low concentration of the paramagnetic impurity. However, upon brief exposure to air, the increasing concentration of 1a• could be visualized as the solution turned deep violet. Accordingly, cyclic voltammograms of 1aH solutions feature the reversible peak of the [1a•/1a<sup>+</sup>] couple at  $E_{1/2} = -1.2$  V vs Fc/Fc<sup>+</sup> (Figure 2a). Importantly, they also show a more intense wave at  $E_{pa} = -0.8$  V, which we attribute to the oxidation of 1aH. No reversibility could be evidenced for this electrochemical wave, even at high sweep rates (up to 10 V s<sup>-1</sup>). In the second cycle of the voltammetry

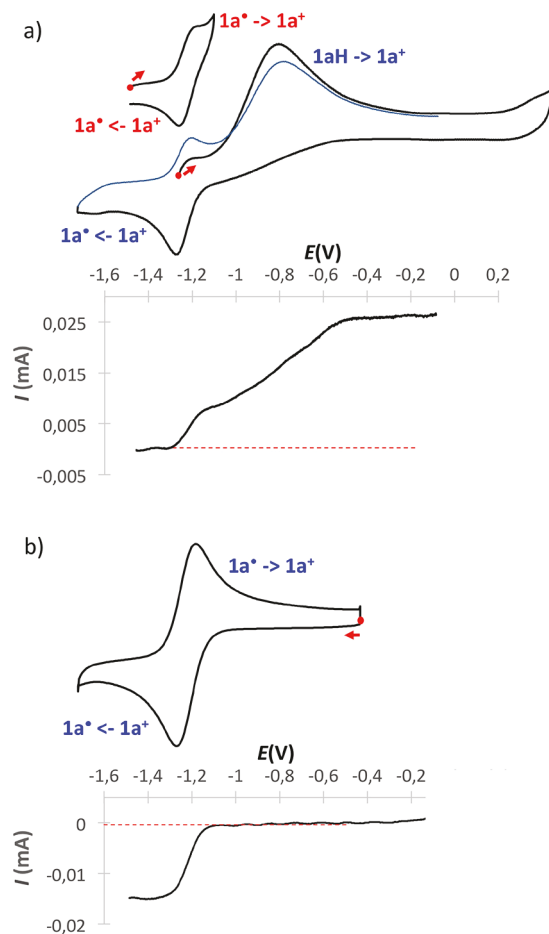


**Figure 2.** Cyclic voltammograms of a solution of **1aH** with the impurity **1a<sup>•</sup>** in  $\text{CH}_3\text{CN} + (\text{nBu})_4\text{NPF}_6$  0.1 mol  $\text{L}^{-1}$  (carbon electrode,  $\Phi = 3$  mm; scan rate: 100 mV  $\text{s}^{-1}$ ;  $E$  vs  $\text{Fc}/\text{Fc}^+$ ) before (a) and after (b) quantitative electrolysis at  $-0.1$  V and the corresponding rotating disk electrode voltammetry studies (RDE; 600 rpm; scan rate: 5 mV  $\text{s}^{-1}$ ).

experiment, this wave decreases in favor of the  $[\text{1a}^{\bullet}/\text{1a}^+]$  peak, suggesting that the SET from **1aH** triggers a very fast proton transfer and a second SET to yield **1a<sup>+</sup>**. To confirm this hypothesis, we performed a quantitative electrochemical oxidation of this solution at  $E = -0.1$  V (Figure 2b). Cyclic voltammetry of the resulting solution was consistent with the disappearance of **1aH** and the formation of **1a<sup>+</sup>**. Rotating disk electrode (RDE) experiments confirmed the convergent oxidations of both **1a<sup>•</sup>** and **1aH** into **1a<sup>+</sup>**, including a significant increase of the Levich limit current for the  $[\text{1a}^{\bullet}/\text{1a}^+]$  couple upon electrolysis.

Next, we turned our attention to enol **2aH**. First, we synthesized the corresponding acylium salt **2a<sup>+</sup>** from NHC **3**<sup>25</sup> and cinnamoyl chloride (Scheme 5). The cyclic voltammogram of **2a<sup>+</sup>** showed two successive reductions at  $E_{1/2} = -0.84$  and  $-1.7$  V, which we attributed to the formation of **2a<sup>•</sup>** and **2a<sup>-</sup>**, respectively (see Figure 3a). This hypothesis was confirmed by the generation of radical **2a<sup>•</sup>** by electrochemical reduction of **2a<sup>+</sup>** at  $E = -1.2$  V. The stoichiometry (one coulomb per mole of reagent), as well as the cyclic voltammogram (similar to that of the starting material), are consistent with a one-electron process with no further chemical transformations. The isotropic EPR spectrum (See Figure 5) of the resulting solution gave definitive evidence for the formation of **2a<sup>•</sup>**.

**Scheme 5. Synthesis of **2a<sup>+</sup>**, and Relationship between Its Different Redox Forms**

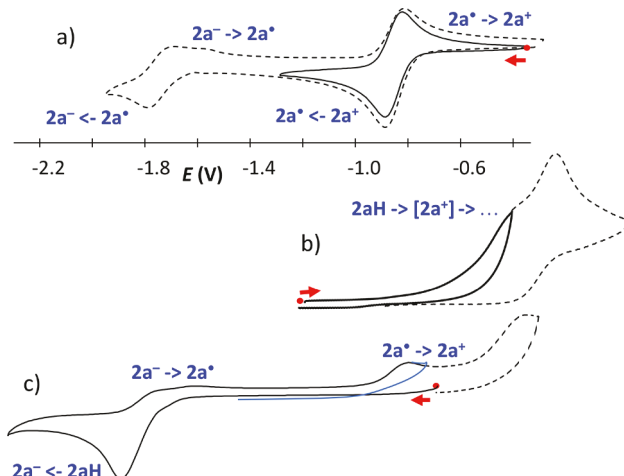
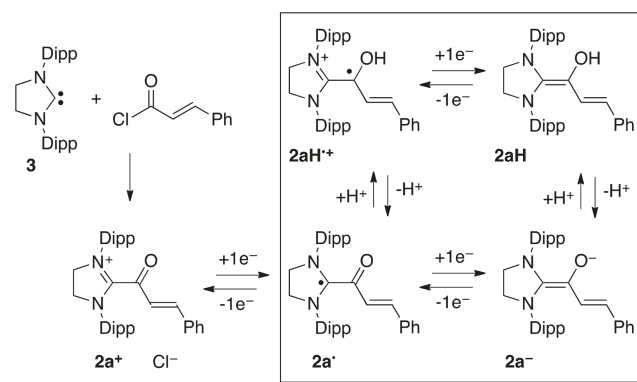


**Figure 3.** (a) Cyclic voltammograms of a solution of **2a<sup>+</sup>**. (b) Cyclic voltammograms of a solution of **2aH** (oxidation first). (c) Cyclic voltammograms of a solution of **2aH** (reduction first) [ $\text{tetrahydrofuran} + (\text{nBu})_4\text{NPF}_6$  0.1 mol  $\text{L}^{-1}$ ; carbon electrode,  $\Phi = 3$  mm; scan rate: 100 mV  $\text{s}^{-1}$ ;  $E$  vs  $\text{Fc}/\text{Fc}^+$ ].

Having characterized **2a<sup>•</sup>**, we performed a cyclic voltammetry study of **2aH**, the corresponding surrogate for Breslow intermediates **IIH**. Similarly to **1aH**, we observed an irreversible oxidation wave at  $E_{\text{pa}} = -0.5$  V (Figure 3b). By analogy, we considered that **2aH** undergoes an overall two-electron oxidation/deprotonation process to afford acylium **2a<sup>+</sup>**. However, the oxidation of **2aH** does not result in the appearance of a current wave for the rereduction of **2a<sup>+</sup>** into **2a<sup>•</sup>** at  $E_{1/2} = -0.84$  V. Interestingly, when initiating the cyclic voltammetry by a reduction of **2aH** (up to  $-2.5$  V, Figure 3c), an irreversible reduction wave is observed at  $E_{\text{pc}} = -1.9$  V. This can be interpreted as the formation of enolate **2a<sup>-</sup>**, as confirmed by the appearance of the expected one-electron reoxidation waves for the formation of **2a<sup>•</sup>** and **2a<sup>+</sup>** at  $E_{\text{pa}} = -1.7$  and  $-0.8$  V, respectively. In this case, again, no rereduction wave of **2a<sup>+</sup>** into **2a<sup>•</sup>** could be seen, thereby indicating that the oxidation of **2a<sup>•</sup>** is followed by a fast chemical transformation. These data demonstrate that the electrophilic acylium **2a<sup>+</sup>** is short-lived in the presence of an excess of the nucleophilic enol **2aH**. Accordingly, neither the quantitative electrochemical oxidations of **2aH** at  $-0.5$  V, nor those at  $-0.2$  V, afford **2a<sup>+</sup>**, but rather yield unidentified products. Importantly, all solutions resulting from the electrochemical oxidation of **2aH** were EPR silent, suggesting

an ionic process for the transformation of the transiently formed acylium  $2\mathbf{a}^+$ .

As a whole, our data invalidate the previously proposed SET from Breslow intermediates to very mild oxidants: nitrostyrenes ( $E_p^{\text{red}} < -1.0$  V versus  $\text{Fc}/\text{Fc}^+$ ),<sup>8a,26</sup> paranitrobenzyl bromide ( $E_p^{\text{red}} \approx -1.2$  V),<sup>8b</sup> pyridine oxides ( $E_p^{\text{red}} < -0.9$  V),<sup>10a,11</sup> nitrobenzenes ( $E_p^{\text{red}} < -0.9$  V),<sup>12</sup> as well as nitrobenzenesulfonic carbamate ( $E_p^{\text{red}} \approx -1.2$  V).<sup>10b</sup> Enols  $1\mathbf{a}\mathbf{H}$  and  $2\mathbf{a}\mathbf{H}$  ( $E_{1/2} = -0.8$  and  $-0.5$  V, respectively) are not strong enough reductants for these substrates. Additionally, these surrogates are rather electron-rich, due to their imidazolidine scaffold. As the catalytically relevant Breslow intermediates of type **IH** or **IIH** are more electron-poor, their oxidation should require even higher potentials. This reasonable assumption is supported by the reported electrochemical properties of compounds **4**–**6** (see Figure 4).<sup>3b,16c</sup> In

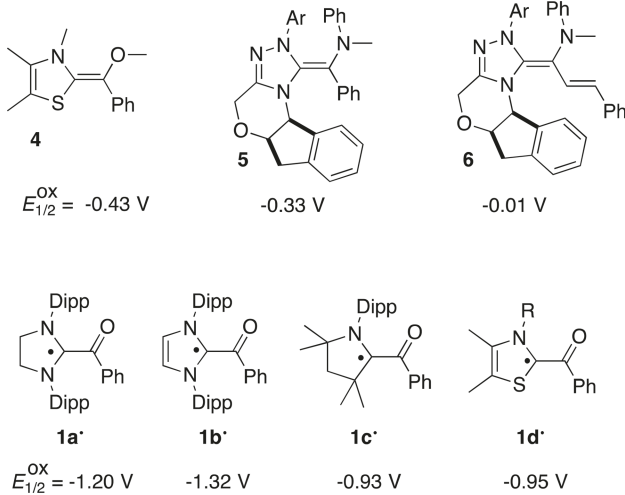


**Figure 4.** Reversible one-electron oxidation potential (versus  $\text{Fc}/\text{Fc}^+$ ) of surrogates for Breslow intermediates and of various NHC-based (amino)(carboxy) C-radicals.

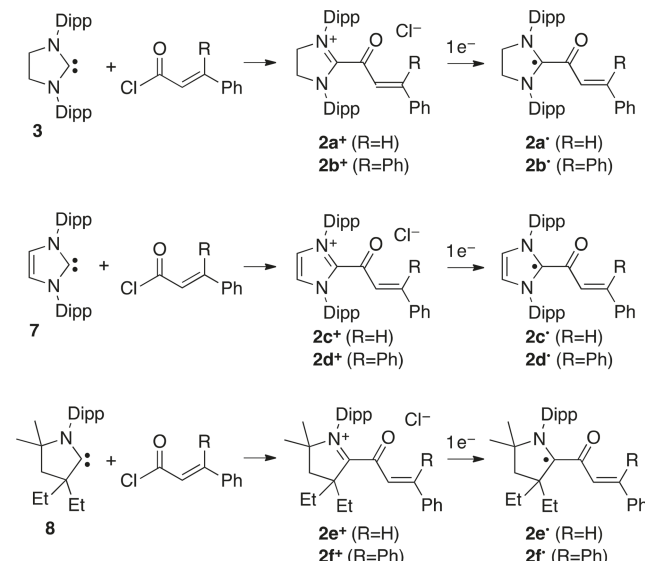
these models for Breslow intermediates, the reactive OH moiety is replaced by a methoxy or an amino group. They all undergo oxidation above  $-0.5$  V.<sup>27</sup> Note that we reported a similar trend for radical derivatives **1a**–**d**· (Figure 4), whose oxidation potentials ( $E_{1/2}^{\text{ox}}$  for  $1\mathbf{b}^{\cdot} < 1\mathbf{a}^{\cdot} < 1\mathbf{d}^{\cdot} < 1\mathbf{c}^{\cdot}$ ) parallel the electron-withdrawing capabilities of the corresponding NHC component ( $1\mathbf{b}^{\cdot} < 1\mathbf{a}^{\cdot} < 1\mathbf{d}^{\cdot} < 1\mathbf{c}^{\cdot}$ ).<sup>28</sup>

Not only is SET irrelevant at low potentials, but the subsequent loss of an electron would not lead to a significant concentration of radicals. Indeed, the one-electron oxidation of these enols triggers a fast deprotonation, and, at the potential that is required for the oxidation of  $1\mathbf{a}^{\cdot}\mathbf{H}$  and  $2\mathbf{a}^{\cdot}\mathbf{H}$ , the resulting radicals  $1\mathbf{a}^{\cdot}$  and  $2\mathbf{a}^{\cdot}$  are readily oxidized into acyliums  $1\mathbf{a}^+$  and  $2\mathbf{a}^+$ , respectively. A concerted proton–electron transfer from Breslow intermediates, which would act as formal  $\text{H}^{\bullet}$  donors, could account for the formation of radicals in oxidative NHC catalysis. Alternatively, when reactions occur in very basic media, the enolate forms  $\text{I}^-$  and  $\text{II}^-$  could act as strong one-electron reductants. In any case, for NHC-catalyzed radical transformations of enols, the relevant intermediate is not **IIH**·+, as previously believed, but is the neutral (amino)(carboxy) C-radicals **II**·.

Radical  $2\mathbf{a}^{\cdot}$  decayed within hours, even under strictly inert conditions. Looking for an isolable version, we extended the

series and synthesized acyliums  $2\mathbf{b}$ – $\mathbf{f}^+$ , from the reaction of cinnamoyl and 3,3-diphenylacryloyl chlorides with imidazolidinylidene **3**, imidazolylidene **7**,<sup>25</sup> and cyclic (alkyl)(amino)carbene **8**<sup>29</sup> (Scheme 6).

**Scheme 6.** Synthesis of Azoliums  $2\mathbf{a}$ – $\mathbf{f}^+$  and One-Electron Reduction into Corresponding Radicals  $2\mathbf{a}$ – $\mathbf{f}^{\cdot}$



The cyclic voltammograms of these acyliums feature two reduction peaks, which are attributed to the formation of the radical and enolate species, respectively (Table 1). While the

**Table 1.** Redox Potentials and Mulliken Spin Densities of Radicals  $2\mathbf{a}$ – $\mathbf{f}^{\cdot}$

$\mathbf{X}^{\bullet}$	$2\mathbf{a}^{\cdot}$	$2\mathbf{b}^{\cdot}$	$2\mathbf{c}^{\cdot}$	$2\mathbf{d}^{\cdot}$	$2\mathbf{e}^{\cdot}$	$2\mathbf{f}^{\cdot}$
$E_{1/2}$ (V) <sup>a</sup>						
$\mathbf{X}^{\bullet}/\mathbf{X}^+$	-0.84	-0.90	-0.92	-0.97	-0.47	-0.53
$\mathbf{X}^-/\mathbf{X}^{\bullet}$	-1.8 <sup>b</sup>	-1.7 <sup>b</sup>	-1.93	-1.93	-1.5 <sup>b</sup>	-1.5 <sup>b</sup>
% Spin Density <sup>c</sup>						
on N <sup>d</sup>	14.2	13.0	19.7	17.6	19.6	19.1
on C1	31.1	33.3	20.0	21.2	40.0	41.1
on C2	11.9	11.2	12.5	12.7	7.2	5.9
on O1	29.0	29.0	26.3	27.1	26.1	27.2
on C3	-11.9	-11.8	-11.8	-12.2	-7.6	-6.0
on C4	20.6	19.9	24.2	24.2	12.8	10.8

<sup>a</sup> $E$  vs  $\text{Fc}/\text{Fc}^+$ . <sup>b</sup> $E_{\text{pc}}$  for an irreversible electrochemical process.

<sup>c</sup>Mulliken spin densities. <sup>d</sup>Sum of spin density on all nitrogen atoms.

first process is electrochemically reversible, the second reduction is coupled to a chemical transformation (i.e., the formation of the corresponding enols).<sup>19d</sup> We then carried out the electrochemical syntheses. In all cases, the stoichiometry (one coulomb per mole of reagent) was consistent with a one-electron process, and cyclic voltammograms were similar for the final and the starting solutions. As expected, room-temperature EPR spectra of the corresponding solutions featured strong signals at  $g \approx 2.0$ . Hyperfine coupling constants could be extracted by mathematical fitting,<sup>24</sup> apart for the unresolved broad band of  $2\mathbf{b}^{\cdot}$  (Figure 5).

As observed with  $2\mathbf{a}^{\cdot}$ , radicals  $2\mathbf{b}$ – $\mathbf{d}^{\cdot}$  decayed within hours and could not be isolated. In contrast, electrochemically prepared CAAC-based radicals  $2\mathbf{e}^{\cdot}$  and  $2\mathbf{f}^{\cdot}$  are persistent for

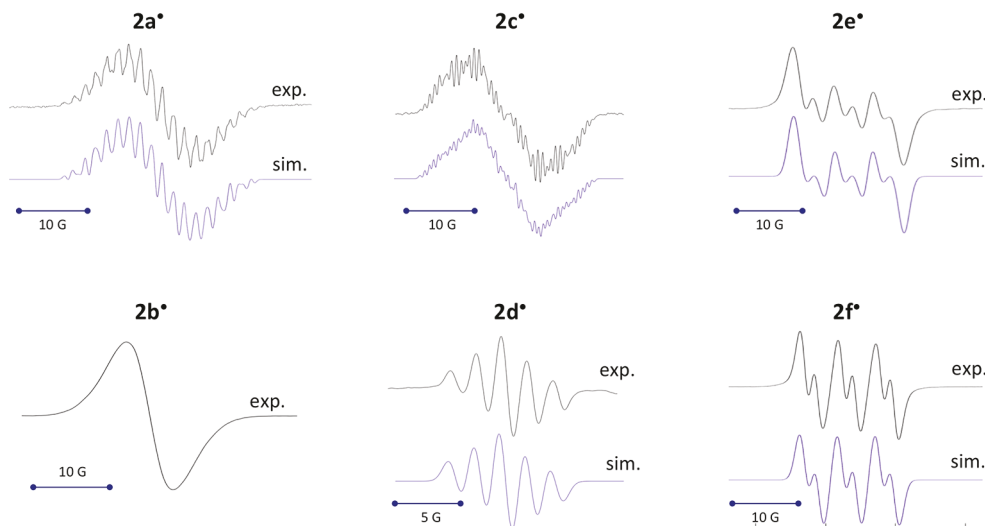


**Figure 5.** Experimental X-band EPR spectra of **2a–f** in solution at room temperature. The hyperfine structure of the spectrum of **2b<sup>•</sup>** could not be resolved. In the other cases, the simulated band shapes are represented for the following set of parameters (*lw*, Lorentzian line-broadening; *a*, hyperfine coupling constants): **2a<sup>•</sup>**, *lw* = 0.085, *a*(<sup>14</sup>N) = 2.5 and 4.4 MHz, *a*(<sup>1</sup>H) = 12.3, 5.1, 8.4 (2 nuclei), 10.3 (2 nuclei), and 3.3 MHz (2 nuclei); **2c<sup>•</sup>**, *lw* = 0.042, *a*(<sup>14</sup>N) = 6 MHz (2 nuclei), *a*(<sup>1</sup>H) = 11.8, 4.1, 4.3, 3.0 (2 nuclei), 2.1 (2 nuclei), and 1.5 MHz (2 nuclei); **2d<sup>•</sup>**, *lw* = 0.15, *a*(<sup>14</sup>N) = 5.4 MHz (2 nuclei); **2e<sup>•</sup>**, *lw* = 0.2, *a*(<sup>14</sup>N) = 14.9 MHz, *a*(<sup>1</sup>H) = 6.8 and 3.1 MHz; **2f<sup>•</sup>**, *lw* = 0.25, *a*(<sup>14</sup>N) = 14.9 MHz, and *a*(<sup>1</sup>H) = 7.1 MHz.

several days in solution under air- and moisture-free conditions. Thus, we carried out their chemical synthesis by reacting the corresponding acyliums **2e<sup>+</sup>** and **2f<sup>+</sup>** with 0.5 equiv of Zinc(0) powder. After workup, **2e<sup>•</sup>** and **2f<sup>•</sup>** were isolated in 47% and 57% yield, respectively. Single crystals of **2f<sup>+</sup>** and **2f<sup>•</sup>** for X-ray analysis were also obtained (Figure 6).<sup>30</sup> As

short C3–C4 double bonds (135.4 and 135.8 pm), suggesting that **2f<sup>•</sup>** has negligible spin density on those atoms.

We performed DFT calculations to gain more insight into the electronic structure of these radicals. We chose the uB3LYP/TZVP level of theory, which already proved to be suitable for (amino)(carboxy) C-radicals.<sup>19</sup> Importantly, the optimized structure of **2f<sup>•</sup>**, as well as the predicted isotropic Fermi constants for radicals **2a<sup>•</sup>** and **2c–e<sup>•</sup>**, fit well with the experimental values (see the Supporting Information). As expected, the Mulliken spin density was reminiscent of push–pull C-centered (amino)(carboxy) radicals with a large portion of the spin densities on C1 and O1. As suggested by the experimental structural data, only 11% spin density is on the C4 carbon atom of **2f<sup>•</sup>**. This radical is essentially described by the resonance forms **2f<sub>I</sub><sup>•</sup>** and **2f<sub>II</sub><sup>•</sup>**, with a smaller contribution from the zwitterionic form **2f<sub>III</sub><sup>•</sup>** (see Figure 7). In contrast, radicals **2a–d<sup>•</sup>** feature up to 25% of the spin density at the C4 carbon atom. Thus, it is likely that their decay results from radical reactivity at this position. Conversely, lower spin densities at this position must contribute to the longer lifetime

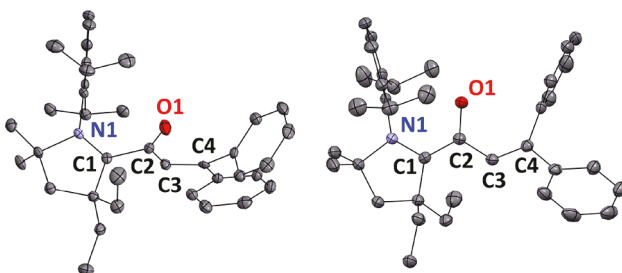


**Figure 6.** Left, solid-state structure of **2f<sup>+</sup>** with thermal ellipsoids drawn at 50% probability level. Hydrogen atoms are omitted for clarity. Selected bond lengths [pm], angles [deg], and torsions [deg]: N1–C1, 128.6(4); C1–C2, 152.2(4); C2–O1, 121.3(4); C2–C3, 145.3(5); C3–C4, 135.8(4); N1–C1–C2, 122.5(3); C1–C2–C3, 115.0(3); C2–C3–C4, 124.8(3); N1–C1–C2–O1, 77.9(4); C1–C2–C3–C4, 174.4(3); right, solid-state structure of **2f<sup>•</sup>** with thermal ellipsoids drawn at 50% probability level. Selected bond lengths [pm], angles [deg], and torsions [deg]: N1–C1, 136.9(1); C1–C2, 141.5(2); C2–O1, 130.0(1); C2–C3, 146.4(2); C3–C4, 135.4(2); N1–C1–C2, 122.1(1); C1–C2–C3, 120.2(1); C2–C3–C4, 127.5(1); N1–C1–C2–O1, −8.2(2); C1–C2–C3–C4, 180.0(1).

previously observed for related (amino)(benzoxo)radicals,<sup>19</sup> the carbene unit of acylium **2f<sup>+</sup>** is nearly orthogonal to the carbonyl moiety, whereas the corresponding radical **2f<sup>•</sup>** has a fully conjugated  $\pi$ -system, with coplanar N1, C1, O1, C2, C3, and C4 atoms. The extended conjugation also results in a significantly shorter C1–C2 bond (**2f<sup>+</sup>**, 152.2 pm; **2f<sup>•</sup>**, 141.5 pm). However, the enone moiety in **2f<sup>•</sup>** remains almost unchanged as compared to **2f<sup>+</sup>**. Indeed, both compounds feature long single C2–C3 bonds (146.4 and 145.3 pm) and

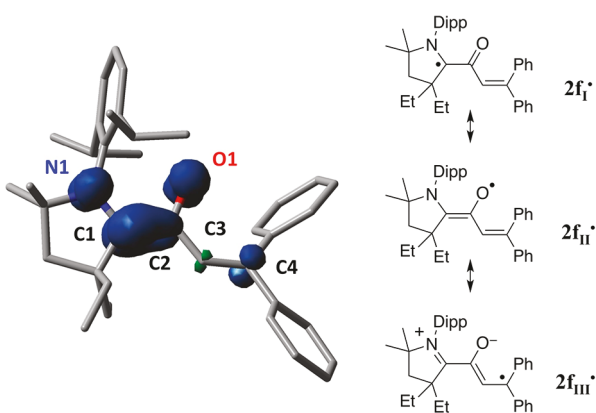


**Figure 7.** Left, representation of computed spin density of **2f<sup>•</sup>**; right, relevant resonance forms.

of CAAC-based radicals **2e**• and **2f**•. Of note, the spin density at C4 is insensitive to substitution (H or Ph substituents), whereas it increases (10–12% for **2e**• and **2f**•; 20% for **2a**• and **2b**•; 24% for **2c**• and **2d**•) when decreasing the  $\pi$ -accepting capability of the carbene unit ( $8 \ll 3 < 7$ ).<sup>28</sup> As a consequence of increased spin delocalization on the C3–C4 moiety, the C2–C3 bonds contract (calculated values for **2e**• and **2f**•, 147.5 pm > **2a**•, 146.0 pm and **2b**•, 145.6 pm > **2c**•, 145.5 pm and **2d**•, 145.0 pm). Concomitantly, the C3–C4 bonds elongate (in the cinnamoyl series, calculated values for **2e**•, 134.5 pm < **2a**•, 135.2 pm and < **2c**•, 135.5 pm; in the diphenylacryloyl series, calculated values for **2f**•, 135.5 pm < **2b**•, 136.3 pm < **2d**•, 136.8 pm).

## CONCLUSION

To account for the fate of several NHC-catalyzed transformations in the presence of mild oxidants, it had been assumed that Breslow intermediates could undergo a single electron transfer below  $-1.0$  V versus  $\text{Fc}/\text{Fc}^+$ . The electrochemical study of electron-rich enols **1aH** and **2aH** definitely rules out this hypothesis. The understanding of these reactions has to now be re-established in light of this novel paradigm.

We showed that the one-electron oxidation of the enols triggers a fast deprotonation, and it occurs at potentials that promote subsequent oxidation leading to the corresponding acyliums **I**<sup>+</sup> and **II**<sup>+</sup>. Therefore, it is likely that the relevant radical intermediates are radicals **I**• and **II**•, and not the previously postulated radical cations **IH**<sup>•+</sup> and **IIH**<sup>•+</sup>. Their formation at low potential may either result from a SET from the corresponding enolates or from a direct  $\text{H}^\bullet$  transfer. However, although radicals have been observed in the course of NHC-catalyzed reactions, there is no definitive evidence that they are genuine intermediates in NHC-catalysis. The set of persistent radicals **2a–f**• could be useful to probe mechanistic hypotheses and explore new reactivities. In particular, CAAC-based radicals not only provide isolable surrogates, but they are excellent redox models because their oxidation potentials are close to the catalytically relevant thiazoylidene-based counterparts.

The impact of this work goes beyond molecular chemistry, as biologic systems raise similar issues. Indeed, highly persistent radical intermediates have been evidenced in mixtures of thiamine-based enzymes and their substrates.<sup>31</sup> Here again, the development of small molecular models is critical for addressing further, not only the genuine nature of the paramagnetic compounds, but also their possible role in biological catalytic cycles, in off-path processes, or in metabolic dysfunctions.

## EXPERIMENTAL SECTION

**General Considerations.** All manipulations were performed under an inert atmosphere of dry argon, using standard Schlenk techniques. Dry and oxygen-free solvents were employed. Stable carbenes were prepared as previously reported.<sup>25,29</sup> <sup>1</sup>H, <sup>13</sup>C, and <sup>19</sup>F NMR spectra were recorded on Bruker Advance 300, Varian VX 500, and Jeol ECA 500 spectrometers. Chemical shifts are given relative to  $\text{SiMe}_4$  and referenced to the residual solvent signal. Melting points were measured with a Büchi Melting Point B-545 apparatus. Electrochemical experiments were carried out with a Biologic SP-300 potentiostat. An  $\text{Ag}/0.01$  M  $\text{AgNO}_3$  reference electrode in  $\text{CH}_3\text{CN} + 0.1$  M  $[\text{nBu}_4\text{N}]^+\text{PF}_6^-$  was used. Cyclic voltammetry experiments were performed in  $\text{CH}_3\text{CN} + 0.1$  M  $[\text{nBu}_4\text{N}]^+\text{PF}_6^-$ , a vitreous carbon disk (3 mm in diameter) as working electrode and a platinum wire as auxiliary electrode. Ferrocene was used as standard,

and all reduction potentials are reported with respect to the  $E_{1/2}$  of the  $\text{Fc}/\text{Fc}^+$  redox couple. Electrochemical reductions were performed using reticulated vitreous carbon electrode. EPR spectra were obtained using an X-band Bruker EMX Plus spectrometer and fitted with the EasySpin simulation package.<sup>24</sup>

### General Procedure for the Synthesis of Acylium Salts **2a–f**<sup>+</sup>.

In a typical procedure, a solution of the carbene (about 1.0 mmol) in diethyl ether (15 mL) was added dropwise to a solution of the acyl chloride (1 equiv) in diethyl ether (10 mL) at 0 °C. The mixture was allowed to warm at room temperature and stirred for an additional hour. After filtration of the supernatant, the precipitate was washed with diethyl ether (3 × 15 mL) and dried in vacuo.

**Chloride Salt of **2a**<sup>+</sup>.** The general procedure was followed with carbene 3 (462 mg, 1.2 mmol) and cinnamoyl chloride (195 mg, 1.2 mmol). White solid. Recrystallization by layering diethyl ether on a concentrated solution in dichloromethane. Yield: 395 mg (64%). mp: 154 °C (dec.). MS (m/z): [M<sup>+</sup>] calcd for  $\text{C}_{36}\text{H}_{45}\text{N}_2\text{O}$ , 521.3526; found, 521.3529. <sup>1</sup>H NMR ( $\text{CDCl}_3$ , 300 MHz):  $\delta$  = 8.12 (d,  $J$  = 16.2 Hz, 1H), 7.61 (d,  $J$  = 7.5 Hz, 2H), 7.36 (m, 5H), d,  $J$  = 7.8 Hz, 2H), 6.36 (d,  $J$  = 16.2 Hz, 1H), 4.94 (s, 4H), 3.38 (sept,  $J$  = 6.6 Hz, 4H), 1.33 (d,  $J$  = 6.6 Hz, 12H), 1.19 (d,  $J$  = 6.6 Hz, 12H). <sup>13</sup>C NMR ( $\text{CDCl}_3$ , 75 MHz):  $\delta$  = 178.4, 162.1, 153.1 (CH), 146.8, 133.4 (CH), 132.6, 131.6 (CH), 130.1 (CH), 129.3 (CH), 128.9, 125.3 (CH), 120.0 (CH), 55.3 (CH<sub>2</sub>), 29.2 (CH), 26.5 (CH<sub>3</sub>), 23.4 (CH<sub>3</sub>).

**Chloride Salt of **2b**<sup>+</sup>.** The general procedure was followed with carbene 3 (357 mg, 0.9 mmol) and 3,3-diphenylacryloyl chloride (220 mg, 0.9 mmol). Yellow solid. Yield: 412 mg (91%). mp: 204 °C (dec.). MS (m/z): [M<sup>+</sup>] calcd for  $\text{C}_{42}\text{H}_{49}\text{N}_2\text{O}$ , 597.3839; found, 597.3838. <sup>1</sup>H NMR ( $\text{CDCl}_3$ , 300 MHz, major conformer):  $\delta$  = 7.52 (t,  $J$  = 7 Hz, 2H), 7.3 (m, 8H), 7.01 (t,  $J$  = 8 Hz, 2H), 6.94 (d,  $J$  = 7.5 Hz, 2H), 6.24 (s, 2H), 6.22 (s, 1H), 4.96 (s, 4H), 3.13 (sept,  $J$  = 7 Hz, 4H), 1.39 (d,  $J$  = 7 Hz, 12H), 1.22 (d,  $J$  = 7 Hz, 12H). <sup>13</sup>C NMR ( $\text{CDCl}_3$ , 75 MHz, major conformer):  $\delta$  = 175.7, 166.4, 162.3, 146.8, 139.0, 136.7, 132.3 (CH), 131.8 (CH), 129.9 (CH), 129.2 (CH), 128.8 (CH), 128.7 (CH), 128.2 (CH), 125.4 (CH), 124.9 (CH), 117.1 (CH), 55.5 (CH<sub>2</sub>), 29.5 (CH), 26.4 (CH<sub>3</sub>), 23.3 (CH<sub>3</sub>).

**Chloride Salt of **2c**<sup>+</sup>.** The general procedure was followed with carbene 7 (469 mg, 1.2 mmol) and cinnamoyl chloride (201 mg, 1.2 mmol). Yellow solid. Yield: 470 mg (70%). mp: 160 °C (dec.). MS (m/z): [M<sup>+</sup>] calcd for  $\text{C}_{36}\text{H}_{43}\text{N}_2\text{O}$ , 519.3370; found, 519.3370. <sup>1</sup>H NMR ( $\text{CDCl}_3$ , 300 MHz):  $\delta$  = 8.89 (s, 2H), 7.64 (d,  $J$  = 15 Hz, 1H), 7.63 (s, 2H), 7.4 (m, 5H), 7.3 (m, 3H), 7.01 (d,  $J$  = 7.5 Hz, 2H), 6.17 (d,  $J$  = 15 Hz, 1H), 2.37 (sept,  $J$  = 7 Hz, 4H), 1.29 (d,  $J$  = 7 Hz, 12H), 1.14 (d,  $J$  = 7 Hz, 12H). <sup>13</sup>C NMR ( $\text{CDCl}_3$ , 75 MHz):  $\delta$  = 173.2, 150.6 (CH), 144.4, 139.1, 133.2 (CH), 132.7, 132.4 (CH), 130.9, 130.2 (CH), 129.4 (CH), 129.2 (CH), 125.2 (CH), 119.1 (CH), 29.4 (CH), 24.8 (CH<sub>3</sub>), 23.2 (CH<sub>3</sub>).

**Chloride Salt of **2d**<sup>+</sup>.** The general procedure was followed with carbene 7 (325 mg, 0.8 mmol) and 3,3-diphenylacryloyl chloride (203 mg, 0.8 mmol). Yellow solid. Yield: 340 mg (64%). mp: 213 °C. MS (m/z): [M<sup>+</sup>] calcd for  $\text{C}_{42}\text{H}_{47}\text{N}_2\text{O}$ , 595.3683; found, 595.3682. <sup>1</sup>H NMR ( $\text{CDCl}_3$ , 300 MHz):  $\delta$  = 8.80 (s, 2H), 7.67 (t,  $J$  = 8 Hz, 2H), 7.42 (d,  $J$  = 8 Hz, 4H), 7.3 (m, 6H), 6.7 (m, 4H), 6.23 (s, 1H), 2.43 (sept,  $J$  = 7 Hz, 4H), 1.33 (d,  $J$  = 7 Hz, 12H), 1.19 (d,  $J$  = 7 Hz, 12H). <sup>13</sup>C NMR ( $\text{CDCl}_3$ , 75 MHz):  $\delta$  = 172.1, 165.7, 144.8, 141.1, 139.6, 136.6, 132.3 (CH), 131.9 (CH), 130.5, 129.9 (CH), 129.1 (CH), 129.0 (CH), 128.6 (CH), 128.1 (CH), 125.1 (CH), 118.3 (CH), 29.5 (CH), 25.3 (CH<sub>3</sub>), 23.0 (CH<sub>3</sub>).

**Chloride Salt of **2e**<sup>+</sup>.** The general procedure was followed with carbene 8 (404 mg, 1.3 mmol) and cinnamoyl chloride (202 mg, 1.2 mmol). White solid. Recrystallization by layering diethyl ether on a concentrated solution in dichloromethane. Yield: 430 mg (74%). mp: 139 °C (dec.). MS (m/z): [M<sup>+</sup>] calcd for  $\text{C}_{31}\text{H}_{42}\text{NO}$ , 444.3261; found, 444.3263. <sup>1</sup>H NMR ( $\text{CDCl}_3$ , 300 MHz):  $\delta$  = 7.9 (m, 3H), 7.85 (d,  $J$  = 11 Hz, 1H), 7.4 (m, 4H), 7.28 (s, 1H), 7.27 (d,  $J$  = 11 Hz, 1H), 3.14 (sept,  $J$  = 6 Hz, 2H), 2.69 (s, 2H), 2.34 (m, 4H), 1.69 (s, 6H), 1.35 (d,  $J$  = 6 Hz, 6H), 1.19 (d,  $J$  = 6 Hz, 6H), 1.08 (t,  $J$  = 7.5 Hz, 6H). <sup>13</sup>C NMR ( $\text{CDCl}_3$ , 75 MHz):  $\delta$  = 195.6, 184.1, 149.9 (CH), 145.6, 133.1 (CH), 132.7, 131.8 (CH), 131.0 (CH), 129.3 (CH),

127.5, 126.3 (CH), 120.6 (CH), 84.6 (C), 58.9 (C), 43.2 (CH<sub>2</sub>), 29.7 (CH<sub>2</sub>), 29.4 (CH), 29.1 (CH), 26.3 (CH<sub>3</sub>), 24.7 (CH<sub>3</sub>), 8.1 (CH<sub>3</sub>).

**Chloride Salt of 2f<sup>t</sup>.** The general procedure was followed with carbene 8 (270 mg, 0.8 mmol) and 3,3-diphenylacryloyl chloride (195 mg, 0.8 mmol). Yellow solid. Recrystallization by layering diethyl ether on a concentrated solution in dichloromethane. Yield: 430 mg (65%). mp: 165 °C. MS (*m/z*): [M<sup>+</sup>] calcd for C<sub>37</sub>H<sub>46</sub>NO, 520.3574; found, 520.3577. <sup>1</sup>H NMR (CDCl<sub>3</sub>, 300 MHz):  $\delta$  = 7.60 (t, *J* = 7 Hz, 1H), 7.4 (m, 8H), 7.17 (t, *J* = 7 Hz, 2H), 7.10 (s, 1H), 6.45 (d, *J* = 7 Hz, 2H), 2.96 (sept, *J* = 6 Hz, 2H), 2.75 (s, 2H), 2.40 (sept, *J* = 7 Hz, 2H), 2.08 (sept, *J* = 7 Hz, 2H), 1.72 (s, 6H), 1.31 (d, *J* = 6 Hz, 6H), 1.12 (t, *J* = 7 Hz, 6H), 0.99 (d, *J* = 6 Hz, 6H). <sup>13</sup>C NMR (CDCl<sub>3</sub>, 75 MHz):  $\delta$  = 194.5, 182.6, 166.3, 146.2, 138.4, 137.6, 132.6 (CH), 132.1 (CH), 130.2 (CH), 129.6 (CH), 129.1 (CH), 128.9 (CH), 128.4 (CH), 128.2, 126.7 (CH), 118.1 (CH), 84.9, 59.0, 43.0 (CH<sub>2</sub>), 29.7 (CH<sub>2</sub>), 29.6 (CH), 29.5 (CH), 26.0 (CH<sub>3</sub>), 25.5 (CH<sub>3</sub>), 9.3 (CH<sub>3</sub>).

**Synthesis of Radicals 2e<sup>•</sup> and 2f<sup>•</sup>.** THF (25 mL) was added once to a Schlenk tube containing the acylium (1 equiv) and activated zinc powder (0.6 equiv) at room temperature. The mixture was allowed to stir for additional 2 h. The solvent was evaporated, and the product was extracted with diethyl ether (3  $\times$  10 mL). Volatiles were removed in vacuo, affording dark green powders. 2e<sup>•</sup> was synthesized according to this general procedure, from 267 mg (0.55 mmol) of chloride salts of 2e<sup>+</sup>. Yield: 115 mg (47%). mp: 64–66 °C. 2f<sup>•</sup> was synthesized according to this general procedure from 500 mg (0.90 mmol) of chloride salts of 2f<sup>+</sup>. Yield: 267 mg (57%). mp: 54–66 °C. Suitable monocrystals for X-ray analysis were grown by cooling a concentrated pentane solution at –40 °C.

## ■ ASSOCIATED CONTENT

### Supporting Information

The Supporting Information is available free of charge on the ACS Publications website at DOI: [10.1021/jacs.8b11824](https://doi.org/10.1021/jacs.8b11824).

<sup>1</sup>H and <sup>13</sup>C NMR spectra of all new compounds, additional voltammograms, computational details, and X-ray crystallographic data ([PDF](#))

X-ray crystallographic data for compound 2a<sup>+</sup> ([CIF](#))

## ■ AUTHOR INFORMATION

### Corresponding Authors

\*[david.martin@univ-grenoble-alpes.fr](mailto:david.martin@univ-grenoble-alpes.fr)  
\*[guybertrand@ucsd.edu](mailto:guybertrand@ucsd.edu)

### ORCID

Rodolphe Jazza: [0000-0002-4156-7826](https://orcid.org/0000-0002-4156-7826)

Guy Bertrand: [0000-0003-2623-2363](https://orcid.org/0000-0003-2623-2363)

David Martin: [0000-0002-3257-9876](https://orcid.org/0000-0002-3257-9876)

### Notes

The authors declare no competing financial interest.

## ■ ACKNOWLEDGMENTS

This work was supported by the French-American cultural exchange foundation (FACE), the NSF (CHE-1661518), and the French National Agency for Research (ANR-14-CE06-0013-01 and ANR-17-ERC2-0015). Thanks are due to the University of Grenoble-Alpes, including the Agir-Pole fund, the LabEx ARCANE fund (ANR-11-LABX-0003-01), the “investissement d’avenir” programm (ANR-15-IDEX-02) for an international mobility grant for V.R., the “Centre de Calcul Intensif en Chimie de Grenoble”, and the ICMG Chemistry Nanobio Platform of Grenoble. E.A.R. benefited from a GAANN fellowship from the U.S. Department of Education.

## ■ REFERENCES

- (1) Breslow, R. On the Mechanism of Thiamine Action. IV. Evidence from Studies on Model Systems. *J. Am. Chem. Soc.* **1958**, *80*, 3719.
- (2) (a) Ukai, T.; Tanaka, R.; Dokawa, T. A new catalyst for acyloin condensation. *J. Pharm. Soc. Jpn.* **1943**, *63*, 296. (b) Stetter, H.; Rämsch, R. Y.; Kuhlmann, H. Über die präparative Nutzung der Thiazoliumsalz-katalysierten Acyloin- und Benzoin-Bildung, I. Herstellung von einfachen Acyloinen und Benzoinen. *Synthesis* **1976**, *1976*, 733.
- (3) For other early studies on thiamine related intermediates, see: (a) Jordan, F.; Kudzin, Z. H.; Rios, C. B. Generation and physical properties of enamines related to the key intermediate in thiamin diphosphate-dependent enzymic pathways. *J. Am. Chem. Soc.* **1987**, *109*, 4415. (b) Barletta, G.; Chung, A. C.; Rios, C. B.; Jordan, F.; Schlegel, M. Electrochemical oxidation of enamines related to the key intermediate on thiamin diphosphate dependent enzymic pathways: evidence for one-electron oxidation via a thiazolium cation radical. *J. Am. Chem. Soc.* **1990**, *112*, 8144.
- (4) For recent reviews on stable carbenes, see: (a) Hahn, F. E.; Jahnke, M. C. Heterocyclic Carbenes: Synthesis and Coordination Chemistry. *Angew. Chem., Int. Ed.* **2008**, *47*, 3122. (b) Melaimi, M.; Soleilhavoup, M.; Bertrand, G. Stable Cyclic Carbenes and Related Species beyond Diaminocarbenes. *Angew. Chem., Int. Ed.* **2010**, *49*, 8810. (c) Martin, D.; Soleilhavoup, M.; Bertrand, G. Stable singlet carbenes as mimics for transition metal centers. *Chem. Sci.* **2011**, *2*, 389. (d) Slaughter, L. M. Acyclic Aminocarbenes in Catalysis. *ACS Catal.* **2012**, *2*, 1802. (e) Hopkinson, M. N.; Richter, C.; Schedler, M.; Glorius, F. An overview of N-heterocyclic carbenes. *Nature* **2014**, *510*, 485. (f) Melaimi, M.; Jazza, R.; Soleilhavoup, M.; Bertrand, G. Cyclic (Alkyl)(amino)carbenes (CAACs): Recent Developments. *Angew. Chem., Int. Ed.* **2017**, *56*, 10046.
- (5) For thematic issues and books on stable carbenes, see: (a) Rovis, T.; Nolan, S. P. Stable Carbenes: From ‘Laboratory Curiosities’ to Catalysis Mainstays. *Synlett* **2013**, *24*, 1188. (b) Arduengo, A. J.; Bertrand, G. Carbenes Introduction. *Chem. Rev.* **2009**, *109*, 3209. (c) *N-Heterocyclic Carbene in Transition Metal Catalysis and Organocatalysis*; Cazin, C. S. J., Ed.; Springer: London, 2011. (d) *N-Heterocyclic Carbenes: From Laboratory Curiosities to Efficient Synthetic Tools*; Díez-González, S., Ed.; Royal Society of Chemistry Publishing: Cambridge, 2011. (e) *N-Heterocyclic Carbenes—Effective Tools for Organometallic Synthesis*; Nolan, S. P., Ed.; Wiley-VCH: Weinheim, 2014. (f) Hahn, F. E. Introduction: Carbene Chemistry. *Chem. Rev.* **2018**, *118*, 9455.
- (6) (a) Enders, D.; Niemeier, O.; Henseler, A. Organocatalysis by N-Heterocyclic Carbenes. *Chem. Rev.* **2007**, *107*, 5606. (b) Grossmann, A.; Enders, D. N-Heterocyclic Carbene Catalyzed Domino Reactions. *Angew. Chem., Int. Ed.* **2012**, *51*, 314. (c) Vora, H. U.; Wheeler, P.; Rovis, T. Exploiting Acyl and Enol Azolium Intermediates via N-Heterocyclic Carbene-Catalyzed Reactions of  $\alpha$ -Reducible Aldehydes. *Adv. Synth. Catal.* **2012**, *354*, 1617. (d) Bugaut, X.; Glorius, F. Organocatalytic umpolung: N-heterocyclic carbenes and beyond. *Chem. Soc. Rev.* **2012**, *41*, 3511. (e) Izquierdo, J.; Hutson, G. E.; Cohen, D. T.; Scheidt, K. A. A Continuum of Progress: Applications of N-Heterocyclic Carbene Catalysis in Total Synthesis. *Angew. Chem., Int. Ed.* **2012**, *51*, 11686. (f) Ryan, S. J.; Candish, L.; Lupton, D. W. Acyl anion free N-heterocyclic carbene organocatalysis. *Chem. Soc. Rev.* **2013**, *42*, 4906. (g) Flanigan, D. M.; Romanov-Michailidis, F.; White, N. A.; Rovis, T. Organocatalytic Reactions Enabled by N-Heterocyclic Carbenes. *Chem. Rev.* **2015**, *115*, 9307. (h) Menon, R. S.; Biju, A. T.; Nair, V. Recent advances in N-heterocyclic carbene (NHC)-catalysed benzoin reactions. *Beilstein J. Org. Chem.* **2016**, *12*, 444. (i) Ren, Q.; Li, M.; Yuan, L.; Wang, J. Recent advances in N-heterocyclic carbene catalyzed achiral synthesis. *Org. Biomol. Chem.* **2017**, *15*, 4731.
- (7) See also: (a) De Sarkar, S.; Biswas, A.; Samanta, R. C.; Studer, A. Catalysis with N-Heterocyclic Carbenes under Oxidative Conditions. *Chem. - Eur. J.* **2013**, *19*, 4664. (b) Mahatthananchai, J.; Bode, J. W. On the Mechanism of N-Heterocyclic Carbene-Catalyzed Reactions

Involving Acyl Azoliums. *Acc. Chem. Res.* **2014**, *47*, 696. (c) Zhang, C.; Hooper, J. F.; Lupton, D. W. N-Heterocyclic Carbene Catalysis via the  $\alpha,\beta$ -Unsaturated Acyl Azolium. *ACS Catal.* **2017**, *7*, 2583. (d) Guin, J.; De Sarkar, S.; Grimme, S.; Studer, A. Biomimetic Carbene-Catalyzed Oxidations of Aldehydes Using TEMPO. *Angew. Chem., Int. Ed.* **2008**, *47*, 8727. (e) De Sarkar, S.; Grimme, S.; Studer, A. NHC Catalyzed Oxidations of Aldehydes to Esters: Chemo-selective Acylation of Alcohols in Presence of Amines. *J. Am. Chem. Soc.* **2010**, *132*, 1190.

(8) (a) Du, Y.; Wang, Y.; Li, X.; Shao, Y.; Li, G.; Webster, R. D.; Chi, Y. R. N-Heterocyclic Carbene Organocatalytic Reductive  $\beta,\beta$ -Coupling Reactions of Nitroalkenes via Radical Intermediates. *Org. Lett.* **2014**, *16*, 5678. (b) Li, B.-S.; Wang, Y.; Proctor, R. S. J.; Zhang, Y.; Webster, R. D.; Yang, S.; Song, B.; Chi, Y. R. Carbene-catalysed reductive coupling of nitrobenzyl bromides and activated ketones or imines via single-electron-transfer process. *Nat. Commun.* **2016**, *7*, 12933. (c) Wang, Y.; Du, Y.; Huang, X.; Wu, X.; Zhang, Y.; Yang, S.; Chi, Y. R. Carbene-Catalyzed Reductive Coupling of Nitrobenzyl Bromide and Nitroalkene via the Single-Electron-Transfer (SET) Process and Formal 1,4-Addition. *Org. Lett.* **2017**, *19*, 632. (d) Wang, Y.; Wu, X.; Chi, Y. R. Synthesis of indanes via carbene-catalyzed single-electron-transfer processes and cascade reactions. *Chem. Commun.* **2017**, *53*, 11952.

(9) See also: (a) Yang, W.; Hu, W.; Dong, X.; Li, X.; Sun, J. N-Heterocyclic Carbene Catalyzed  $\gamma$ -Dihalomethylation of Enals by Single-Electron Transfer. *Angew. Chem., Int. Ed.* **2016**, *55*, 15783. (b) Wu, X.; Zhang, Y.; Wang, Y.; Ke, J.; Jeret, M.; Reddi, R. N.; Yang, S.; Song, B.-A.; Chi, Y. R. Polyhalides as Efficient and Mild Oxidants for Oxidative Carbene Organocatalysis by Radical Processes. *Angew. Chem., Int. Ed.* **2017**, *56*, 2942. (c) Zhao, K.; Enders, D. Merging N-Heterocyclic Carbene Catalysis and Single Electron Transfer: A New Strategy for Asymmetric Transformations. *Angew. Chem., Int. Ed.* **2017**, *56*, 3754.

(10) (a) White, N. A.; Rovis, T. Enantioselective N-Heterocyclic Carbene-Catalyzed  $\beta$ -Hydroxylation of Enals Using Nitroarenes: An Atom Transfer Reaction That Proceeds via Single Electron Transfer. *J. Am. Chem. Soc.* **2014**, *136*, 14674. (b) Zhang, Y.; Du, Y.; Huang, Z.; Xu, J.; Wu, X.; Wang, Y.; Wang, M.; Yang, S.; Webster, R. D.; Chi, Y. R. N-Heterocyclic Carbene-Catalyzed Radical Reactions for Highly Enantioselective  $\beta$ -Hydroxylation of Enals. *J. Am. Chem. Soc.* **2015**, *137*, 2416.

(11) White, N. A.; Rovis, T. Oxidatively Initiated NHC-Catalyzed Enantioselective Synthesis of 3,4-Disubstituted Cyclopentanones from Enals. *J. Am. Chem. Soc.* **2015**, *137*, 10112.

(12) Cheng, X.-Y.; Chen, K.-Q.; Sun, D. Q.; Ye, S. N-Heterocyclic carbene-catalyzed oxidative [3 + 2] annulation of dioxindoles and enals: cross coupling of homoenolate and enolate. *Chem. Sci.* **2017**, *8*, 1936.

(13) (a) Schmittel, M.; Baumann, U. Stability and Cyclization of Enol Radical Cations: A Mechanistic Study of One-Electron Oxidation of  $\beta,\beta$ -Dimesityl Enols. *Angew. Chem., Int. Ed. Engl.* **1990**, *29*, 541. (b) Schmittel, M.; Röck, M. Enol cation radicals in solution. 3. Reaction of enol cation radicals in the presence of nucleophiles. *Chem. Ber.* **1992**, *125*, 1611. (c) Röck, M.; Schmittel, M. Enol cation radicals in solution. 4. An improved Synthesis of 4,6,7-Trimethylbenzofurans by oxidation of  $\beta$ -mesityl substituted enols. *J. Prakt. Chem./Chem.-Ztg.* **1994**, *336*, 325. (d) Schmittel, M.; Gescheidt, G.; Röck, M. The First Spectroscopic Identification of an Enol Radical Cation in Solution: The Anisyl-dimesitylethenol Radical Cation. *Angew. Chem., Int. Ed. Engl.* **1994**, *33*, 1961. (e) Schmittel, M.; Lal, M.; Lal, R.; Röck, M.; Langels, A.; Rappoport, Z.; Basheer, A.; Schlirf, J.; Deiseroth, H.-J.; Flörke, U.; Gescheidt, G. A comprehensive picture of the one-electron oxidation chemistry of enols, enolates and  $\alpha$ -carbonyl radicals: oxidation potentials and characterization of radical intermediates. *Tetrahedron* **2009**, *65*, 10842.

(14) (a) Dixon, W. T.; Murphy, D. Determination of the acidity constants of some phenol radical cations by means of electron spin resonance. *J. Chem. Soc., Faraday Trans. 2* **1976**, *72*, 1221. (b) Brede, O.; Orthner, H.; Zubarev, V.; Hermann, R. Radical Cations of Sterically Hindered Phenols as Intermediates in Radiation-Induced Electron Transfer Processes. *J. Phys. Chem.* **1996**, *100*, 7097.

(15) Nakanishi, I.; Itoh, S.; Fukuzumi, S. Electron-Transfer Properties of Active Aldehydes of Thiamin Coenzyme Models, and Mechanism of Formation of the Reactive Intermediates. *Chem. - Eur. J.* **1999**, *5*, 2810.

(16) (a) Teles, J. H.; Melder, J.-P.; Ebel, K.; Schneider, R.; Gehrer, E.; Harder, W.; Brode, S.; Enders, D.; Breuer, K.; Raabe, G. The Chemistry of Stable Carbenes. Part 2. Benzoin-type condensations of formaldehyde catalyzed by stable carbenes. *Helv. Chim. Acta* **1996**, *79*, 61. (b) Berkessel, A.; Elfert, S.; Etzenbach-Effers, K.; Teles, J. H. Aldehyde Umpolung by N-Heterocyclic Carbenes: NMR Characterization of the Breslow Intermediate in its Keto Form, and a Spiro-Dioxolane as the Resting State of the Catalytic System. *Angew. Chem., Int. Ed.* **2010**, *49*, 7120. (c) DiRocco, D. A.; Oberg, K. M.; Rovis, T. Isolable Analogues of the Breslow Intermediate Derived from Chiral Triazolylidene Carbenes. *J. Am. Chem. Soc.* **2012**, *134*, 6143. (d) DiRocco, D. A.; Rovis, T. Catalytic Asymmetric Cross-Aza-Benzoin Reactions of Aliphatic Aldehydes with N-Boc-Protected Imines. *Angew. Chem., Int. Ed.* **2012**, *51*, 5904. (e) Magi, B.; Mayr, H. Structures and Reactivities of O-Methylated Breslow Intermediates. *Angew. Chem., Int. Ed.* **2012**, *51*, 10408. (f) Colett, C. J.; Massey, R. S.; Maguire, O. R.; Batsanov, A. S.; O'Donoghue, A. C.; Smith, A. D. Mechanistic insights into the triazolylidene-catalysed Stetter and benzoin reactions: role of the N-aryl substituent. *Chem. Sci.* **2013**, *4*, 1514. (g) Martin, D.; Canac, Y.; Lavallo, V.; Bertrand, G. Comparative Reactivity of Different Types of Stable Cyclic and Acyclic Mono- and Diamino Carbenes with Simple Organic Substrates. *J. Am. Chem. Soc.* **2014**, *136*, 5023.

(17) Very recently, a thiazolinylidene-based (amino)enol was characterized in solution: Paul, M.; Sudkaow, P.; Wessels, A.; Schlörer, N. E.; Neudörfl, J.-M.; Berkessel, A. Breslow Intermediates from Aromatic N-Heterocyclic Carbenes (Benzimidazolin-2-ylidene, Thiazolin-2-ylidene). *Angew. Chem., Int. Ed.* **2018**, *57*, 8310.

(18) (a) Berkessel, A.; Elfert, S.; Yatham, V. R.; Neudörfl, J.-M.; Schlörer, N. E.; Teles, J. H. Umpolung by N-Heterocyclic Carbenes: Generation and Reactivity of the Elusive 2,2-Diamino Enols (Breslow Intermediates). *Angew. Chem., Int. Ed.* **2012**, *51*, 12370. (b) Berkessel, A.; Yatham, V. R.; Elfert, S.; Neudörfl, J.-M. Characterization of the Key Intermediates of Carbene-Catalyzed Umpolung by NMR Spectroscopy and X-Ray Diffraction: Breslow Intermediates, Homoenolates, and Azolium Enolates. *Angew. Chem., Int. Ed.* **2013**, *52*, 11158.

(19) (a) Martin, D.; Moore, C. E.; Rheingold, A. L.; Bertrand, G. An Air-Stable Oxyallyl Radical Cation. *Angew. Chem., Int. Ed.* **2013**, *52*, 7014. (b) Mahoney, J. K.; Martin, D.; Moore, C. E.; Rheingold, A.; Bertrand, G. Bottleable (Amino)(Carboxy) Radicals Derived from Cyclic (Alkyl)(Amino)Carbenes. *J. Am. Chem. Soc.* **2013**, *135*, 18766. (c) Mahoney, J. K.; Martin, D.; Thomas, F.; Moore, C.; Rheingold, A. L.; Bertrand, G. Air-Persistent Monomeric (Amino)(carboxy) Radicals Derived from Cyclic (Alkyl)(Amino) Carbenes. *J. Am. Chem. Soc.* **2015**, *137*, 7519. (d) Mahoney, J. K.; Jazzar, R.; Royal, G.; Martin, D.; Bertrand, G. The Advantages of Cyclic Over Acyclic Carbenes To Access Isolable Capto-Dative C-Centered Radicals. *Chem. - Eur. J.* **2017**, *23*, 6206. (e) Mahoney, J. K.; Regnier, V.; Romero, E. A.; Molton, F.; Royal, G.; Jazzar, R.; Martin, D.; Bertrand, G. The serendipitous discovery of a readily available redox-bistable molecule derived from cyclic(alkyl)(amino)carbenes. *Org. Chem. Front.* **2018**, *5*, 2073.

(20) Rehbein, J.; Ruser, S.-M.; Phan, J. NHC-catalysed benzoin condensation – is it all down to the Breslow intermediate? *Chem. Sci.* **2015**, *6*, 6013.

(21) DFT calculations were performed with the *Gaussian 09* software package: Frisch, M. J.; Trucks, G. W.; Schlegel, H. B.; Scuseria, G. E.; Robb, M. A.; Cheeseman, J. R.; Scalmani, G.; Barone, V.; Mennucci, B.; Petersson, G. A.; Nakatsuji, H.; Caricato, M.; Li, X.; Hratchian, H. P.; Izmaylov, A. F.; Bloino, J.; Zheng, G.; Sonnenberg, J. L.; Hada, M.; Ehara, M.; Toyota, K.; Fukuda, R.; Hasegawa, J.;

Ishida, M.; Nakajima, T.; Honda, Y.; Kitao, O.; Nakai, H.; Vreven, T.; Montgomery, J. A., Jr.; Peralta, J. E.; Ogliaro, F.; Bearpark, M.; Heyd, J. J.; Brothers, E.; Kudin, K. N.; Staroverov, V. N.; Kobayashi, R.; Normand, J.; Raghavachari, K.; Rendell, A.; Burant, J. C.; Iyengar, S. S.; Tomasi, J.; Cossi, M.; Rega, N.; Millam, N. J.; Klene, M.; Knox, J. E.; Cross, J. B.; Bakken, V.; Adamo, C.; Jaramillo, J.; Gomperts, R.; Stratmann, R. E.; Yazyev, O.; Austin, A. J.; Cammi, R.; Pomelli, C.; Ochterski, J. W.; Martin, R. L.; Morokuma, K.; Zakrzewski, V. G.; Voth, G. A.; Salvador, P.; Dannenberg, J. J.; Dapprich, S.; Daniels, A. D.; Farkas, Ö.; Foresman, J. B.; Ortiz, J. V.; Cioslowski, J.; Fox, D. J. *Gaussian 09*, revision 4.2.0; Gaussian, Inc.: Wallingford, CT, 2009.

(22) (a) Schaefer, A.; Horn, H.; Ahlrichs, R. Fully optimized contracted Gaussian basis sets for atoms Li to Kr. *J. Chem. Phys.* **1992**, *97*, 2571. (b) Schaefer, A.; Huber, C.; Ahlrichs, R. Fully optimized contracted Gaussian basis sets of triple zeta valence quality for atoms Li to Kr. *J. Chem. Phys.* **1994**, *100*, 5829.

(23) (a) Becke, A. D. Density-functional thermochemistry. III. The role of exact exchange. *J. Chem. Phys.* **1993**, *98*, 5648. (b) Lee, C.; Yang, W.; Parr, R. G. Development of the Colle-Salvetti correlation-energy formula into a functional of the electron density. *Phys. Rev. B: Condens. Matter Mater. Phys.* **1988**, *37*, 785. (c) Vosko, S. H.; Wilk, L.; Nusair, M. Accurate spin-dependent electron liquid correlation energies for local spin density calculations: a critical analysis. *Can. J. Phys.* **1980**, *58*, 1200. (d) Stephens, P. J.; Devlin, F. J.; Chabalowski, C. F.; Frisch, M. J. Ab Initio Calculation of Vibrational Absorption and Circular Dichroism Spectra Using Density Functional Force Fields. *J. Phys. Chem.* **1994**, *98*, 11623.

(24) Experimental EPR spectra were fitted with the EasySpin simulation package: Stoll, S.; Schweiger, A. EasySpin, a comprehensive software package for spectral simulation and analysis in EPR. *J. Magn. Reson.* **2006**, *178*, 42.

(25) For the synthesis of *N*-heterocyclic(diamino)carbenes, see: (a) Arduengo, A. J., III; Dias, H. V. R.; Harlow, R. L.; Kline, M. Electronic stabilization of nucleophilic carbenes. *J. Am. Chem. Soc.* **1992**, *114*, 5530. (b) Arduengo, A. J., III; Goerlich, J. R.; Marshall, W. J. A stable diaminocarbene. *J. Am. Chem. Soc.* **1995**, *117*, 11027. (c) Denk, M. K.; Avinash, T.; Hatano, K.; Lough, A. J. Steric Stabilization of Nucleophilic Carbenes. *Angew. Chem., Int. Ed. Engl.* **1997**, *36*, 2607. (d) Arduengo, A. J., III; Krafczyk, R.; Schmutzler, R.; Craig, H. A.; Goerlich, J. R.; Marshall, W. J.; Unverzagt, M. Imidazolylidenes, imidazolinylidenes and imidazolidines. *Tetrahedron* **1999**, *55*, 14523.

(26) For an electrochemical study of nitrostyrenes, see: Squella, J. A.; Sturm, J. C.; Weiss-lopez, B.; Bonta, M.; Nunez-Vergara, L. J. Electrochemical study of  $\beta$ -nitrostyrene derivatives: steric and electronic effects on their electroreduction. *J. Electroanal. Chem.* **1999**, *466*, 90.

(27) Note that the value of  $E_{1/2} = +0.49$  V versus SSCE (about  $-0.1$  V vs  $\text{Fc}/\text{Fc}^+$ ), which was initially measured for **6** (ref 16c), has later been continuously misreported as  $-0.49$  V versus SSCE (about  $-1$  V vs  $\text{Fc}/\text{Fc}^+$ ).

(28) (a) Dröge, T.; Glorius, F. The Measure of All Rings-N-Heterocyclic Carbenes. *Angew. Chem., Int. Ed.* **2010**, *49*, 6940. (b) Back, O.; Henry-Ellinger, M.; Martin, C. D.; Martin, D.; Bertrand, G.  $^{31}\text{P}$  NMR Chemical Shifts of Carbene-Phosphinidene Adducts as an Indicator of the  $\pi$ -Accepting Properties of Carbenes. *Angew. Chem., Int. Ed.* **2013**, *52*, 2939. (c) Liske, A.; Verlinden, K.; Buhl, H.; Schaper, K.; Ganter, C. Determining the  $\pi$ -Acceptor Properties of N-Heterocyclic Carbenes by Measuring the  $^{77}\text{Se}$  NMR Chemical Shifts of Their Selenium Adducts. *Organometallics* **2013**, *32*, 5269. (d) Rodrigues, R. R.; Dosey, C. L.; Arceneaux, C. A.; Hudnall, T. W. Phosphaalkene vs. phosphinidene: the nature of the P-C bond in carbonyl-decorated carbene $\rightarrow$ PPh adducts. *Chem. Commun.* **2014**, *50*, 162. (e) Yummaleti, S. V. C.; Nelson, D. J.; Poater, A.; Gomez-Suarez, A.; Cordes, D. B.; Slawin, A. M. Z.; Nolan, S. P.; Cavallo, L. What can NMR spectroscopy of selenoureas and phosphinidenes teach us about the  $\pi$ -accepting abilities of N-heterocyclic carbenes? *Chem. Sci.* **2015**, *6*, 1895. (f) Deardorff, C. L.; Sikma, E. R.; Rhodes, C. P.; Hudnall, T. W. Carbene-derived  $\alpha$ -acyl formamidinium cations: organic molecules

with readily tunable multiple redox processes. *Chem. Commun.* **2016**, *52*, 9024.

(29) For the synthesis of CAACs, see: (a) Lavallo, V.; Canac, Y.; Präsang, C.; Donnadieu, B.; Bertrand, G. Stable Cyclic (Alkyl)-(Amino)Carbenes as Rigid or Flexible, Bulky, Electron-Rich Ligands for Transition-Metal Catalysts: A Quaternary Carbon Atom Makes the Difference. *Angew. Chem., Int. Ed.* **2005**, *44*, 5705. (b) Jazza, R.; Dewhurst, R. D.; Bourg, J. B.; Donnadieu, B.; Canac, Y.; Bertrand, G. Intramolecular "Hydroiminiumation" of Alkenes: Application to the Synthesis of Conjugate Acids of Cyclic Alkyl Amino Carbenes (CAACs). *Angew. Chem., Int. Ed.* **2007**, *46*, 2899. (c) Jazza, R.; Bourg, J. B.; Dewhurst, R. D.; Donnadieu, B.; Bertrand, G. Intramolecular "Hydroiminiumation and amidiniumation" of Alkenes: A Convenient, Flexible, and Scalable Route to Cyclic Iminium and Imidazolinium Salts. *J. Org. Chem.* **2007**, *72*, 3492. (d) Zeng, X.; Frey, G. D.; Kinjo, R.; Donnadieu, B.; Bertrand, G. Synthesis of a Simplified Version of Stable Bulky and Rigid Cyclic (Alkyl)(amino)carbenes, and Catalytic Activity of the Ensuing Gold(I) Complex in the Three-Component Preparation of 1,2-Dihydroquinoline Derivatives. *J. Am. Chem. Soc.* **2009**, *131*, 8690. (e) Tomás-Mendivil, E.; Hansmann, M. M.; Weinstein, C. M.; Jazza, R.; Melaimi, M.; Bertrand, G. Bicyclic (Alkyl)(amino)carbenes (BICAACs): Stable Carbenes More Ambiphilic than CAACs. *J. Am. Chem. Soc.* **2017**, *139*, 7753.

(30) The X-ray structure of a related acylazolium was previously published: Samanta, R. C.; Maji, B.; De Sarkar, S.; Bergander, K.; Fröhlich, R.; Mück-Lichtenfeld, C.; Mayr, H.; Studer, A. Nucleophilic Addition of Enols and Enamines to  $\alpha,\beta$ -Unsaturated Acyl Azoliums: Mechanistic Studies. *Angew. Chem., Int. Ed.* **2012**, *51*, 5234.

(31) (a) Mansoorabadi, S. O.; Seravalli, J.; Furdui, C.; Krymov, V.; Gerfen, G. J.; Begley, T. P.; Melnick, J.; Ragsdale, S. W.; Reed, G. H. EPR Spectroscopic and Computational Characterization of the Hydroxyethylidene-Thiamine Pyrophosphate Radical Intermediate of Pyruvate:ferredoxin Oxidoreductase. *Biochemistry* **2006**, *45*, 7122. (b) Frank, R. A. W.; Kay, C. W. M.; Hirst, J.; Luisi, B. F. Off-Pathway, Oxygen-Dependent Thiamine Radical in the Krebs Cycle. *J. Am. Chem. Soc.* **2008**, *130*, 1662. (c) Stool, S.; Gunn, A.; Brynda, M.; Sughrue, W.; Kohler, A. C.; Ozarowski, A.; Fisher, A. J.; Lagarias, J. C.; Britt, R. D. Structure of the Biliverdin Radical Intermediate in Phycocyanobilin:ferredoxin Oxidoreductase Identified by High-Field EPR and DFT. *J. Am. Chem. Soc.* **2009**, *131*, 1986. (d) Tittmann, K. Reaction mechanisms of thiamin diphosphate enzymes: redox reactions. *FEBS J.* **2009**, *276*, 2454. (e) Meyer, D.; Neumann, P.; Koers, E.; Sjuts, H.; Lüdtke, S.; Sheldrick, G. M.; Ficner, R.; Tittmann, K. Unexpected tautomeric equilibria of the carbanionenamine intermediate in pyruvate oxidase highlight unrecognized chemical versatility of thiamin. *Proc. Natl. Acad. Sci. U. S. A.* **2012**, *109*, 10867. (f) Nemeria, N. S.; Ambrus, A.; Patel, H.; Gerfen, G.; Adam-Vizi, V.; Tretter, L.; Zhou, J.; Wang, J.; Jordan, F. Human 2-Oxoglutarate Dehydrogenase Complex E1 Component Forms a Thiamin-derived Radical by Aerobic Oxidation of the Enamine Intermediate. *J. Biol. Chem.* **2014**, *289*, 29859. (g) Reed, G. H.; Ragsdale, S. W.; Mansoorabadi, S. O. Radical reactions of thiamin pyrophosphate in 2-oxoacid oxidoreductases. *Biochim. Biophys. Acta, Proteins Proteomics* **2012**, *1824*, 1291.